Thermal Analysis and Simulation of Cryopump Based on CFD Method

Thermal Analysis and Simulation of Cryopump Based on CFD Method

Yueshuai Zhao[a], Lichen Sun, Wei Sun and Rongping Shao

Beijing Institute of Spacecraft Environment Engineering, Beijing 100094, China

[a] Corresponding author: zhaoyueshuai@163.com

Abstract. Based on CFD method, thermal design and numerical simulation of cryopump first array and second array was performed during the cool-down period and the steady state. The analysis of the temperature distribution of the cryopump was made under various conditions，such as operating conditions, the setting of the thermal rods and the thickness of the radiation shield. The const thermal property and variable thermal property was used in this paper to calculate the cool-down process of the cryopump, the effect of the first array structure was also taken into account. Some important results with typical parameters are: The temperature difference of the first array of the cryopump is greatly affected by the working conditions, especially when facing the room temperature vacuum system, the main heat load is concentrated on the baffle; A variable thickness bottom plate can be used to reduce the overall temperature change of the cryopump; The setting of the thermal rods is very useful to reduce the temperature change of the cryopump; The setting of the thermal rods is preferably close to the center of the baffle; If the variable property was not considered, the deviation of the cool-down time is about 24%.

1. Introduction

In large vacuum system, cryopump was usually used as the main pump for obtaining clean vacuum. The cryopump remove gases and vapors from the vacuum chamber by means of condensation and adsorption on the cold faces under 15K. In order to reduce the heat load of the second array, the baffle and radiation shield under 80K (first array) were used[1].

The first array and second array were cooled by Gifford-McMahon cryocooler. For cryopumps, The normal operating temperature of the second array was between 10K and 20K. In this case, the thermal conductivity of oxygen-free copper at 15K can be 15 times higher than at the room temperature[2]. The maximum temperature difference of the second array is usually less than 1K. However, the maximum temperature difference of the first array is much larger, and can reach about 10-20K [3, 4].

In this condition, detail thermal analysis of the cryopump is necessary, especially for the first array. By optimizing the structure of the cryopump, it is possible to reduce the temperature difference of the second array without changing the cryocooler, and obtain a lower average temperature. On the other hand, after optimizing the structure, when designing the cryopump with the same pumping speed, it is possible to select a cryocooler with a smaller cooling power, which is also advantageous for improving economic efficiency.

The simplest method to improve the temperature distribution of the cryopump, especially for the radiation shield and the baffle is increase the thickness. However, this method also greatly increases

the mass of the first array and so as the cool-down time of the cryopump, which needs to be balanced from these two aspects.

In this paper, the steady-state temperature distribution and cooling process of the first array were analyzed for the DN400 cryopump. The computational fluid dynamics (CFD) numerical simulation was used to analyze the heat transfer of the cryopump. Different thickness of the radiation shield and the heat conducting plate was considered, the difference of the thermal conductivity of copper and the different cooling power of the refrigerator at different temperatures were also calculated. A design method was proposed to improve the temperature uniformity of the cryopump.

2. Numerical Simulation Method and Mathematical Model

2.1. Structure and Composition of the Cryopump

The cryopump is mainly composed of G-M cryocooler, pump housing, first array (radiation shield, baffle, thermal rods, thermal plate), second array (including condensation surface and adsorption surface), etc. Shown as Fig. 1. The radiation shield and the baffle mainly remove water vapor; the condensation surface of the second array is mainly used for removing other condensable gases except He, Ne, H_2; the adsorption surface of the second array is adhered with activated carbon, to adsorb the remaining non-condensable gas. The radiation shield, baffle and second array of the cryopump were cooled by the cryocooler. The radiation shield, baffle and second array of the cryopump were made of oxygen-free copper.

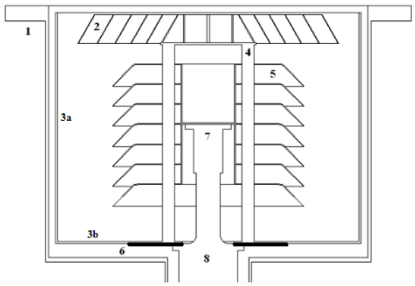

Figure 1. Stucture of DN400 cryopump.

1.Pump housing 2.baffle 3.Radiation shield (3a Shield wall 3b Shield bottom) 4.Thermal rods 5.Second array 6.Thermal plate 7.2nd stage of the cryocooler 8.1st stage of the cryocooler

2.2. Governing Equations

The governing equations for the solid three-dimensional unsteady heat conduction problem is [5]:

$$\frac{\partial(\rho h)}{\partial t} = \nabla \cdot (k \nabla T) \tag{1}$$

where: ρ is density, h is entropy, t is time, k is thermal conductivity, T is temperature.

To simplify the calculation, the radiant heat of the first and second array is calculated directly by the formula (2), and the calculation result of each unit on the wall is connected to the calculation model and substituted as a boundary condition by UDF(User-defined functions):

$$q = \varepsilon_s \sigma \left(T_1^4 - T_2^4 \right) \tag{2}$$

where: q is the heat flux per unit area, ε_s is the system emissivity, σ is the Stefan-Boltzmann constant.

All the surfaces in the cryopump are assumed to be gray surface, and the surface emissivity of each surface is set as follows:

Baffle: 0.9; pump housing (inner surface): 0.1; radiation shield (outer surface): 0.1; radiation shield (inner surface): 0.9; second array condensation surface: 0.1; second array adsorption surface: 0.9. The specific heat capacity and thermal conductivity of copper are temperature dependent[6-7].
The cooling power of the G-M cryocooler was setting as Fig. 2.

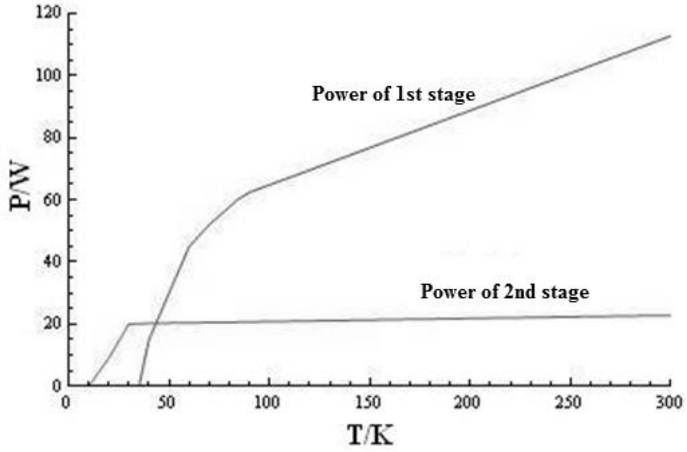

Figure 2. The power of the 1st and 2nd stage of the G-M cryocooler

The physical properties of the material and the cooling parameters of the cryocooler are also connected to the calculation model by means of UDF.

3. Results and Analysis

3.1. The steady Temperature Distribution of the Cryopump

3.1.1. The Steady Temperature Distribution of the Cryopump. Generally, there are mainly three operating conditions when the cryopump was used in a high-vacuum system.
1) Pre-cooling condition: the cryopump and the vacuum system are isolated by the valve;
2) The liquid nitrogen condition: The cryopump operates in a vacuum system with liquid nitrogen heat sink;
3) Room temperature condition: the cryopump operates in a vacuum system at room temperature.
Under case 2) and case 3), The vacuum vessel is usually much larger than the cryopump, the system emissivity can directly adopt the surface emissivity of the baffle.
The three-dimensional steady-state temperature distribution of the first array of the cryopump calculated under different working conditions is shown in Fig. 3.

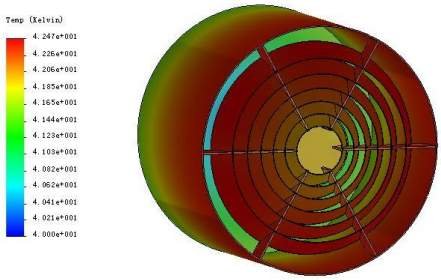

(a)Case 1

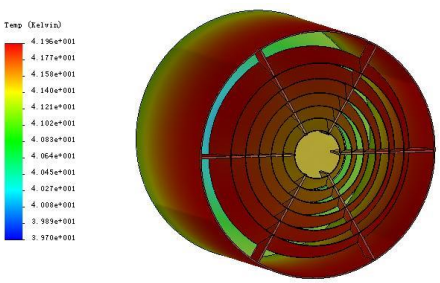

(b)Case 2

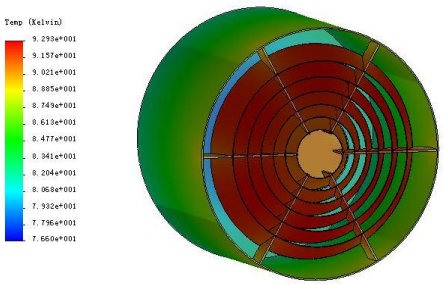

(c)Case 3

Figure 3. The three-dimensional steady-state temperature distribution of the first array of the cryopump calculated under different working conditions

In the pre-cooling condition, the average temperature of the first array is about 41K, and the maximum temperature rise is about 2.5K, as shown in Fig. 3a). In the liquid nitrogen condition, the average temperature of the first array is about 40K, the maximum temperature rise is about 2K, as shown in Fig. 3b). In room temperature condition, the average temperature of the first array is about 85K, and the maximum temperature rise is about 16.3K, as shown in Fig. 3c).

It can be seen from the figure that different operating conditions have a great influence on the temperature distribution of the cryopump. In room temperature condition, the temperature rise of the cryopump is the largest, which is the key point of the optimal design of the cryopump. The hottest part of the cold array takes on the main heat load of the cryopump.

Under room temperature condition, the temperature rise of each part of the cryopump's first array is shown in Fig.4 (the abscissa indicates the distance from the primary refrigerator), and the maximum temperature difference of the shield bottom plate is about 5.6K, The maximum temperature difference of the shield wall is about 6.5K, and the maximum temperature difference of the baffle is about 4.2K.

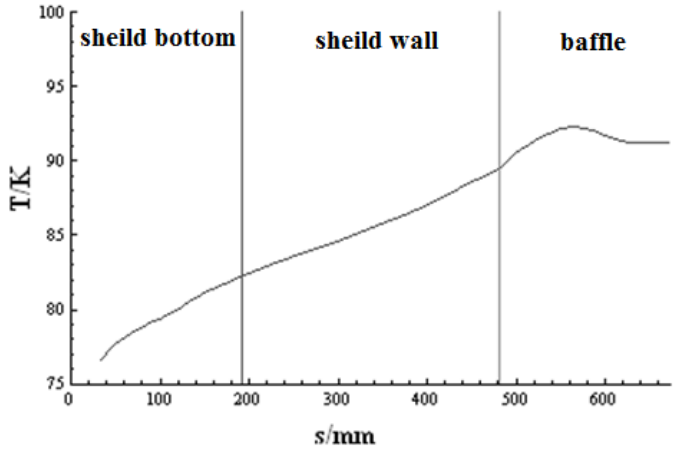

Figure 4. The temperature distribution of each part of the cryopump's first array

3.1.2. Effect of Thermal Rods Setting. In first array of the cryopump, the lowest and the highest temperature parts were connected by several thermal rods.

In order to investigate the effect of the thermal rods on the temperature distribution of the cryopump's first array, three different thermal rods settings were simulated:

Case1: no thermal rod was set;

Case2: 4 thermal rods (10 mm diameter) were set;

Case3: 4 thermal rods (15 mm diameter) were set.

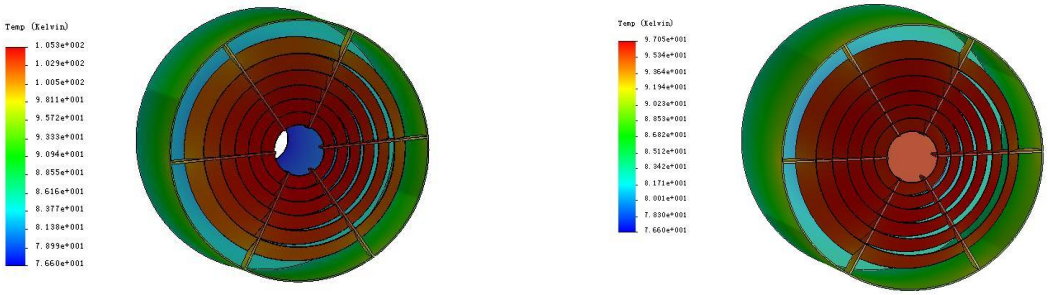

a) Without thermal rods b)With 4-φ10mm thermal rods

Figure 5. The temperature distribution of the first array under different thermal rods setting

In case1, the average temperature of the first array is about 91K, and the maximum temperature rise is about 28.9K, as shown in Fig. 5a); In case2, the average temperature of the first array is about 86.8K, and the maximum temperature rise is about 20.5K, as shown in Fig. 5b); In case3, the temperature distribution is shown in Fig. 3c).
Fig. 6 shows the temperature distribution of the baffle in case1 and case3:

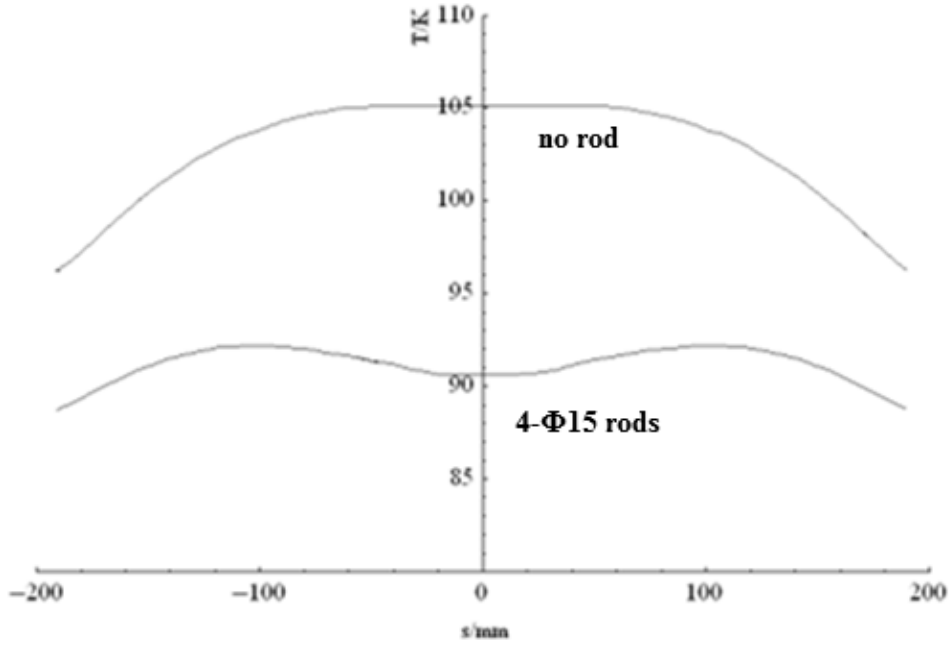

Figure 6. The temperature distribution of the baffle under different thermal rods setting

It can be seen from the figure that the arrangement of the thermal rods greatly reduces the thermal resistance of the baffle to the cryocooler, reduces the overall temperature difference of the cryopump, making the baffle temperature more uniform.

3.1.3. Effect of Thickness of the Radiation Shield. In the design of the cryopump first array, the temperature rise on the radiation shield can account for more than 70% of the total temperature rise, and the thickness of the radiation shield has a great influence on the total temperature rise control of the cryopump. Fig. 7 shows the temperature distribution of the first array with the radiation shield thickness of 1.0 mm and 1.5 mm. The temperature distribution with the radiation shield thickness of 2 mm is shown in Fig.3c). Under the three conditions, the maximum temperature rise of the first array of the cryopump is 21.5K, 18.4K and 16.3K.

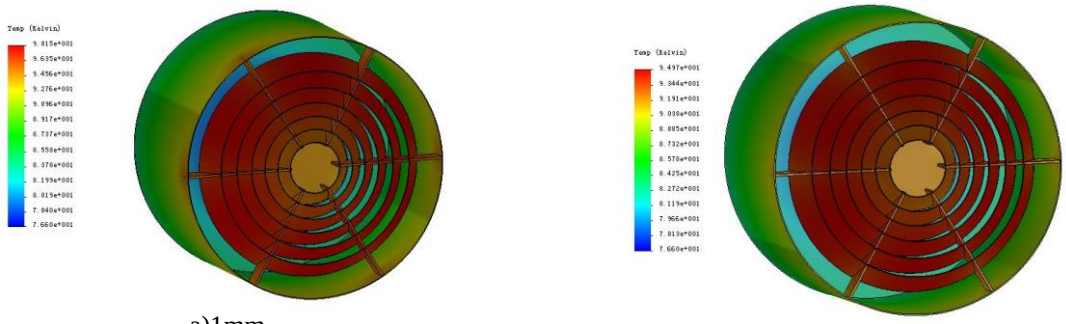

a)1mm b)1.5mm

Figure 7. The temperature distribution of cryopump under different thickness of the radiation shield

Fig. 8 shows the temperature distribution of the radiation shield.

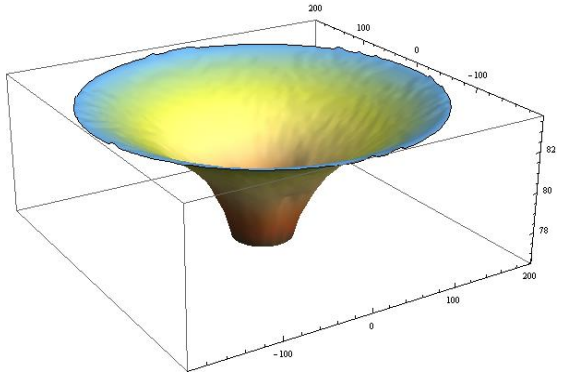

Figure 8. The temperature distribution of the bottom of the radiation shield (Max. 7K)

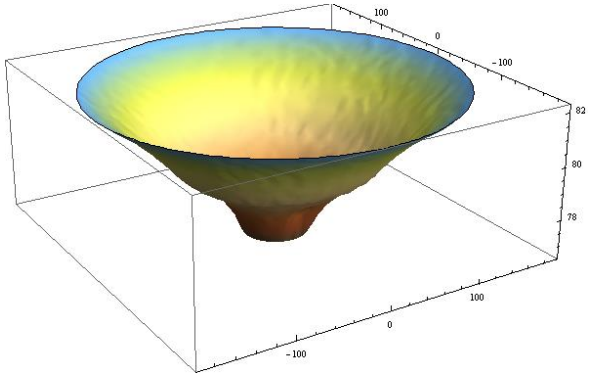

Figure 9. The temperature distribution of the bottom of the radiation shield (Max. 5.6K)

Combined with Fig. 4, it can be seen that the temperature rise of the shield bottom of the radiation shield exhibits a tendency of being fast and slow first. In order to control the temperature rise of the shield bottom plate, thickening the central portion of the bottom plate of the cold screen helps to increase the temperature uniformity of the bottom plate. . As shown in Fig. 9, a thermal plate（2 mm thick） is added to the central portion of the shield bottom plate to reduce the maximum temperature difference of the bottom plate by 1.4K.

3.2. The Temperature of the Cryopump During the Cool-Down Period

3.2.1. Model and Parameter Settings. The cool-down time of the first array of the cryopump refers to the time when the first array is cool-down from room temperature to 100K. The cool-down time of the first array has a great relationship with the thermal load of the cryopump [8-9].

Generally, the finial temperature of the cool-down time of the cryopump is set 20K(which is 10K higher than the equilibrium temperature of the second array), the finial temperature of the cool-down time for the first array is set 10K higher than the balance temperature.

3.2.2. Effects of Constant and Varying Physical Properties. Considering that during the cool-down period of the cryopump, the first array of the cryopump is cooled from 300K to about 40K, and the second array is cooled from 300K to about 10K, the temperature gradient is very large. The selection of the qualitative temperature of the first array and the second array has a great influence on the cooling performance of the cryopump. If the selection is improper, it will generate a large calculation error.
Under the pre-cooling condition, The change of the temperature during the cool-down calculated by the const thermal properties (first array qualitative temperature 170K, second array qualitative temperature 155K) and variable thermal properties was showed as Fig.10.

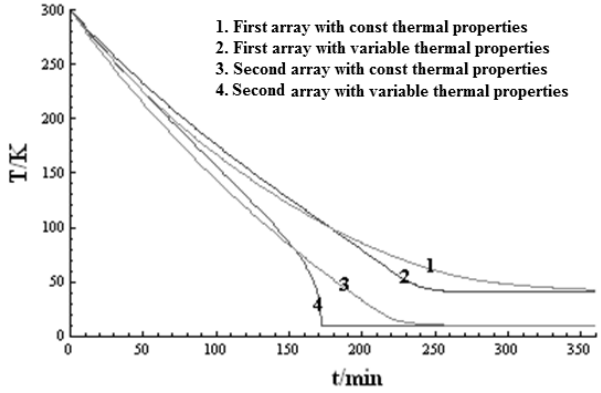

Figure 10. The change of the temperature during the cool-down calculated by the const thermal properties and variable thermal properties

It can be seen from Fig. 12 that the variation in the result calculated by the const thermal properties and variable thermal properties is about 24%. Obviously, if the temperature at the room temperature or the equilibrium temperature was used as the qualitative temperature, the calculation error will become larger.

3.2.3. The Effect of the First Array Structure. Fig.11 shows the cooling curves in three different structural states:
a) no thermal rods, shield wall thickness 1mm;
b) 4 Φ10 thermal rods, shield wall thickness 1.5mm;
c) 4 Φ15mm thermal rods, shield wall thickness 2mm.

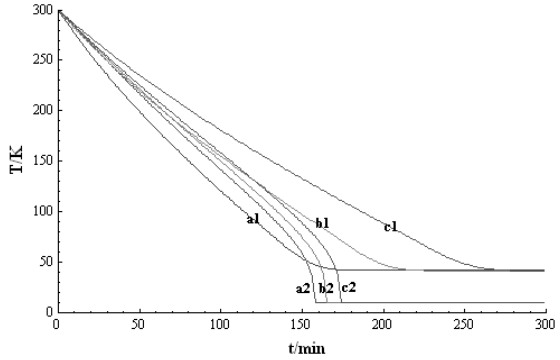

Figure 11. The change of the temperature during the cool-down under different structure of first array

It can be seen from the figure that the cool-down time of the cryopump is prolonged with the increase of the quality of the first array. The cool-down time of the second array of the DN400 cryopump is usually about 100-180 min, within a reasonable range of the cool-down time. It's reasonable to increase the quality of the first array, in order to reduce the thermal resistance and reduce the temperature rise.

4. Conclusion

In this paper, the temperature distribution and temperature drop characteristics of cryopump first and second arrays are studied by numerical simulation. In this study, the thermal conductivity and heat capacity of oxygen-free copper is considered by means of a user defined functions (UDF).
The conclusion can be made as follows:
1) The temperature difference of the first array of the cryopump is much larger than the temperature difference of the second array. The temperature difference of the first array is about 16K, and the temperature difference of the second array is about 1K.
2) The temperature difference of the first array of the cryopump is greatly affected by the working conditions, especially when facing the room temperature vacuum system, the main heat load is concentrated on the baffle;
3) For the bottom plate of the DN400 cryopump, a variable thickness bottom plate or a thermal plate can be used to reduce the overall temperature change of the cryopump;
4) The setting of the thermal rods is very useful to reduce the temperature change of the cryopump. At the same time, according to the temperature distribution of the baffle without the thermal rods, it can be considered that the setting of the thermal rods is preferably close to the center of the baffle;
5) If the variable property was not considered, the deviation of the cool-down time is about 24%。

Acknowledgments
Financial grants from the National Natural Science Foundation of China (NSFC Grant No. U1537109) is gratefully acknowledged.

References

[1] Rogalski A. Progress in focal plane array technologies[C]. Progress in Quantum Electronics. 2012;36(2):342-473.
[2] Kimo M Welch. Recommended practices for measuring the performance and characteristics of closed-loop gaseous helium cryopumps[J]. Journal of Vacuum Science and Technology A, 1999, 17(5):3081-3095.
[3] Baechler, W.G. Cryopumps for research and industry[J]. Vacuum, 1987, 37(1): 21-29.
[4] Johnson V J.Properties of Materials at Low Temperature[M],Pergamon Press,1961.
[5] Baechler WG. Cryopumps for research and industry. Vacuum. 1987;37(1–2):21-9.
[6] Dermois OC, Schmidt PW. A 20 K cryopump with a high conductance baffle design[J]. Vacuum. 1980;30(10):411-4.
[7] Hands BA. Introduction to cryopump design[J]. Vacuum. 1976;26(1):11-6.
[8] Iwasa Y, Ito S. A new type of cryopump with a metal cryopanel cooled below 3.6 K by a two-stage GM refrigerator[J]. Vacuum. 1996;47(6–8):675-8.
[9] Meng D, Sun L, Yan R, Shao R. et al. Effects of cryopump on vacuum helium leak detection system[J]. Vacuum. 2017;143:316-9.